Journal of Hazardous Materials 180 (2010) 289–296

Contents lists available at ScienceDirect

Journal of Hazardous Materials

journal homepage: www.elsevier.com/locate/jhazmat

Effect of sorption kinetics on nickel toxicity in methanogenic granular sludge

Jan Bartacek[a,b,*], Fernando G. Fermoso[a], Alba Beas Catena[a], Piet N.L. Lens[a,b]

[a] Sub-Department of Environmental Technology, Wageningen University, "Biotechnion"-Bomenweg 2, P.O. Box 8129, 6700 EV Wageningen, The Netherlands
[b] Department of Environmental Resources, UNESCO-IHE, P.O. Box 3015, 2601 DA Delft, The Netherlands

ARTICLE INFO

Article history:
Received 10 November 2009
Received in revised form 19 February 2010
Accepted 7 April 2010
Available online 14 May 2010

Keywords:
Nickel toxicity
Metal speciation
Anaerobic granular sludge
Donnan membrane technique
Intra-particle diffusion

ABSTRACT

This study investigates the effect of nickel speciation and its equilibrium kinetics on the nickel toxicity to methylotrophic methanogenic activity. Toxicity tests were done with anaerobic granular sludge in three different media containing variable concentrations of complexing ligands. A correlation between nickel toxicity and the free nickel concentration failed, because not the equilibrium conditions, but the kinetics of the speciation processes taking place in the medium (precipitation, sorption, liquid speciation, etc.) determine nickel bio-uptake and its toxic effect. The latter was confirmed with an *F*-test (*p*-value always lower than 0.1). It was shown that the biological activity (methane production) took place within 3–20 days upon the start of methanogenic experiments, i.e. prior the chemical–physical equilibrium of nickel speciation was established in the methanogenic medium (10–20 days). The process of nickel sorption in the methanogenic granular sludge was limited by intra-particle diffusion and the experimental data fitted to the Weber–Morris sorption model. The other sorption kinetic models applied (pseudo-first order sorption kinetics, pseudo-second order sorption kinetics and first order reversible reaction kinetics) did not fit the experimental data satisfactorily.

1. Introduction

The widely used models for metal toxicity such as the Free Ion Activity Model (FIAM) or the Biotic Ligand Model (BLM) are based on the assumption of chemical–physical equilibrium in the medium. If the equilibrium state is established, toxicity of a given metal can be estimated based on the concentration of any of the metal species present in the medium [1]. Because the free metal ion is always present in the aqueous solution, analytical techniques have intensively focused on the quantification of the free ion concentration [1–3]. However, several interfering phenomena have been recognized, such as the presence of competing metals [1], accumulation of dissolved organic matter (DOM) on the surface of living cells [4], interaction of complexed metals with the cell membrane [5] and limitation of the bio-uptake by metal transport and dissociation [6]. Most importantly, the assumption of the chemical–physical equilibrium is only fulfilled when the physical–chemical processes (sorption, precipitation, chemical speciation, etc.) are slower than the metal transport over the cell membrane [1,7]. In the case that the physical–chemical processes become the rate-limiting step for the bio-uptake, predicting metal toxicity based on the free ion concentration at steady state fails [7].

The interaction between heavy metals and anaerobic granular sludge has been widely studied describing the sorption capacity of the sludge [8], kinetics of the sorption process [9] and the speciation of metals inside the methanogenic granules – solid state speciation [8,10]. However, the implications of these interactions, especially of the speciation equilibrium kinetics, for heavy metal toxicity have not yet been studied in detail.

This study aims to evaluate the effect of nickel liquid phase speciation and its kinetics on nickel toxicity to methylotrophic methanogenesis by anaerobic granular sludge. This was done considering also the crucial effect of nickel sorption kinetics.

2. Materials and methods

2.1. Medium composition

Three different media were prepared with different concentrations of EDTA and phosphates in order to vary the speciation of nickel: medium I contained a high concentration of phosphate and no EDTA, medium II contained both EDTA and phosphate and medium III contained no EDTA and a minimum concentration of phosphate (Table 1). Nickel chloride was used as the nickel source in media I and III. The nickel-EDTA complex ($[NiEDTA]^{2-}$) was prepared from $NiCl_2$ and Na_2H_2EDTA in molar ratio 1:1.5 and supplied into medium II.

* Corresponding author at: Department of Environmental Resources, UNESCO-IHE, P.O. Box 3015, 2601 DA Delft, The Netherlands. Tel.: +31 152 151 880; fax: +31 152 122 921.
E-mail address: j.bartacek@unesco-ihe.org (J. Bartacek).

0304-3894/$ – see front matter © 2010 Elsevier B.V. All rights reserved.
doi:10.1016/j.jhazmat.2010.04.029

Table 1
Differences in the composition of the media used in the present study.

	Phosphate ($mmol\,L^{-1}$)	Carbonate ($mmol\,L^{-1}$)	EDTA ($mmol\,L^{-1}$)
Medium I	1.44	30	0
Medium II	1.44	30	1.5 times the nickel concentration
Medium III	0.14	30	0

Unless specified otherwise, each medium contained (in $mg\,L^{-1}$): NH_4Cl (280), K_2HPO_4 (250), $MgSO_4{\cdot}7H_2O$ (100), $CaCl_2{\cdot}2H_2O$ (10) and $NaHCO_3$ (2520). Moreover, 5 $\mu mol\,L^{-1}$ of Cu, Zn, Mn, Co, Mo, Se and W and 50 $\mu mol\,L^{-1}$ of Fe were added as micronutrients. The pH of media I–III was set to 7.0 with sodium bicarbonate. In the nickel toxicity experiments, nickel additions of 0, 0.1, 0.3, 0.5, 0.6, 0.75, 1.0 and 2.0 $mmol\,L^{-1}$ were supplied in the media. The bottles with the optimal nickel dosage (the bottles with the highest SMA for each medium) were considered as the optimal bottles when evaluating the Hormesis curves and when calculating the nickel toxicity characteristics. All three media were prepared with ultra-pure water (resistivity of 18 MΩ cm, Millipore Corporation, Billerica, Massachusetts, USA).

Although EDTA is usually not present in the UASB reactor influent, this ligand was chosen as an example of a strong, poorly biodegradable ligand [11]. Moreover, EDTA has been used to increase metal bioavailability of essential metals in UASB reactors [12] and its influence can thus be relevant for full-scale UASB reactors. Phosphate was chosen as a weak ligand naturally present in UASB reactors.

In the experiments with pre-incubation, the establishment of the chemical–physical steady state prior to the methanogenic activity was assured by injecting methanol (the sole methanogenic substrate) 30 days after the methanogenic sludge was in contact with the media supplemented with various nickel concentrations.

2.2. Source of biomass

Mesophilic methanogenic granular sludge was obtained from a full-scale UASB reactor treating alcohol distillery wastewater at Nedalco (Bergen op Zoom, The Netherlands). The total suspended solids (TSS) and volatile suspended solids (VSS) concentration of the wet sludge were 6.93 (±0.02) and 6.47 (±0.03)%, respectively. The granular sludge contained 15 (±1) $\mu g\,g\,TSS^{-1}$ Co, 110 (±5) $\mu g\,g\,TSS^{-1}$ Ni, 62 (±1) $\mu g\,g\,TSS^{-1}$ Zn and 8.1 (±1) $mg\,g\,TSS^{-1}$ Fe.

2.3. Specific maximum methanogenic activity tests

The specific methanogenic activity (SMA) with methanol as the substrate was determined in duplicate at 30 (±2) °C using a hand-held pressure meter. The produced pressure was measured 1–3 times a day. Granular sludge specimens (1.00 ± 0.01 g wet wt) were transferred to 120 mL serum bottles containing 50 mL basal medium with methanol (4 g chemical oxygen demand [COD] L^{-1}), along with different nickel concentrations.

2.4. Models for nickel sorption kinetics

Four theoretical models for sorption kinetics were used to fit the experimental data describing nickel sorption on methanogenic granular sludge [13,14]:

(1) Pseudo-first order sorption kinetics

$$q = q_e[1 - \exp(-k_1 t)] \quad (1)$$

where q is the amount of nickel sorbed at time t, q_e is the amount of nickel sorbed at equilibrium (sorption capacity) and k_1 is the kinetic constant. The theoretical concept of this equation is based on the assumption that the driving force of adsorption is linearly proportional to the difference between q_e and q.

(2) Pseudo-second order sorption kinetics

$$\frac{t}{q} = \frac{t}{q_e} + \frac{1}{k_2 q_e^2} \quad (2)$$

where k_2 is the kinetic constant.

(3) First order reversible reaction

$$\ln\left(\frac{C_A - C_e}{C_{A_0} - C_e}\right) = -k_r t \quad (3)$$

where C_A is the concentration of nickel at time t, C_e is the concentration of nickel at equilibrium and C_{A_0} is the initial nickel concentration. k_r is the overall kinetic constant of the reversible chemical reaction (A ⇔ B) that can be considered as a sum of the kinetic constant of both reactions (A → B and B → A).

(4) Weber–Morris sorption model

$$q = k_{WM}\sqrt{t} + I \quad (4)$$

where k_{WM} is the Weber–Morris kinetics constant and I is the intercept describing the fast initial sorption of nickel. The parameters of Weber–Morris model (k_{WM} and I) were calculated from the data obtained before q reached 95% of q_e in each experiment. The Weber–Morris model assumes that the intraparticle diffusion is the process controlling the overall kinetics of the sorption process [13]. In the case that no other processes control the sorption kinetics, the intercept I equals to zero. According to Febrianto et al. [14], the diffusion coefficient within the granules can be calculated (assuming an uniform granule diameter) as follows:

$$D = \frac{\pi}{8640}\left(\frac{d_p k_{WM}}{q_e}\right)^2 \quad (5)$$

where D is the nickel diffusion coefficient and d_p is the granular diameter.

2.5. Statistics for evaluation of the toxicity experiments

The Hormesis model was used to fit the experimental data describing nickel toxicity as described by Bartacek et al. [15]. The parameters of the model were calculated in accordance with Schabenberger et al. [16]:

$$E[y|x] = \delta + \frac{\alpha - \delta + \gamma x}{1 + \theta\ \exp[\beta \ln(x)]} \quad (6)$$

where $E[y|x]$ represents the average response at dosage, α, β, γ and θ are parameters and x is the metal dosage. α was considered as a constant that gives the SMA value when x goes to zero and was determined using the blank bottles; δ was considered as a constant that gives the SMA value at x going to infinity and it was assumed to be 0 $mg\,COD\,(g\,VSS\,d)^{-1}$; γ is responsible for the Hormesis effect, and β and θ are responsible for the slope of the increase or decrease of the curve. The parameters were calculated using nonlinear regression in Microsoft Office Excel® (Thames Valley Park, Reading Berkshire, UK). The main characteristic of the toxicity curves is the concentration causing 50% reduction of the SMA measured in blank (IC_{50}) and the SMA under the optimal conditions (SMA_{max}). These parameters were derived from the Hormesis model.

The toxicity data obtained (IC_{50} and SMA_{max}) were related to the nickel concentration using the statistical analysis described previously [15]. For each medium, a single toxicity curve for each

nickel fraction (added, dissolved and free) was plotted. To decide whether the three curves obtained for a certain fraction are similar among the three sets of experiments, the *F*-test was used with a *p*-value indicating the probability that the three compared curves are identical.

2.6. Dissolved nickel concentration

The dissolved nickel concentration was measured in filtered (pore size of 0.45 μm) samples taken from the system (granular sludge – liquid medium). The liquid medium samples were taken during pre-incubation of the mixture (no substrate added, 30 (±2) °C, anaerobic conditions, shaking at 75 rpm). The value of the dissolved nickel concentration [$c(\mathrm{Ni})_{\mathrm{diss}}$] related to a given supplied amount of nickel [$c(\mathrm{Ni})_{\mathrm{added}}$] was determined after establishing steady state in the bulk solution, as no changes in total dissolved concentration of nickel occurred over a period of several days.

2.7. Determination of nickel sorption

The sorbed nickel fraction was calculated as the difference between the amount of metal added and the total dissolved metal concentration in the medium. It has been previously shown that precipitation and adsorption/absorption of metals in granular sludge cannot be distinguished [17]. Therefore, all the processes coupled with metal transfer between the solid and liquid phase are reported here as overall sorption/precipitation.

2.8. Concentration of free nickel species

The free nickel concentration was determined directly in the granular sludge/medium mixture under anaerobic conditions at 30 (±2) °C using the Donnan membrane technique (DMT) as described by Bartacek et al. [15]. The free nickel (Ni^{2+}) concentrations related to given nickel concentrations in the given system (media I, II, and III) were measured under the same conditions as applied in the SMA experiments, but without substrate.

2.9. Chemical analyses

The nickel concentration was determined by inductively coupled plasma with optical emission spectrometry (Varian, Palo Alto, California, USA) as described by Zandvoort et al. [18]. Values of TSS and VSS concentrations were determined according to APHA/AWWA/WEF [19]. All chemicals were of analytical or biological grade and purchased from Merck (Darmstadt, Germany).

3. Results

3.1. Nickel speciation in granular sludge

3.1.1. Kinetics of nickel sorption/precipitation

Fig. 1a shows the kinetics of nickel sorption/precipitation in the three different media for the nickel addition of 0.3 mmol L^{-1}. While the nickel concentration remained unaffected in medium II, at least 500 h was needed to reach the plateau in media I and III. (1) In contrast, massive sorption/precipitation occurred in media I and III. Especially with the nickel additions lower than 1 mmol L^{-1}, the concentration in the solution (at the end of both the DMT and the toxicity experiments) was as low as 0.001 mmol L^{-1} and more than 99% of the nickel had precipitated. Comparing the nickel concentrations in media I and III at the end of the toxicity tests, slightly higher (1–3 μmol L^{-1}) values were measured in medium I for additions lower than 1 mmol L^{-1}. In contrast, the end-concentrations of nickel were higher in medium III when 1 and 2 mmol L^{-1} of nickel were added (Fig. 1a). The dissolved nickel concentrations at the end of the DMT experiments in medium I were higher than in medium III, except for the two lowest nickel additions (Fig. 1b). The latter was because the dissolved nickel concentrations measured in the DMT experiments in medium I were considerably higher than those measured in the toxicity experiments. In contrast, the dissolved nickel concentrations measured in the DMT experiments in media II and III were approximately as high as those measured in the toxicity experiments using these media.

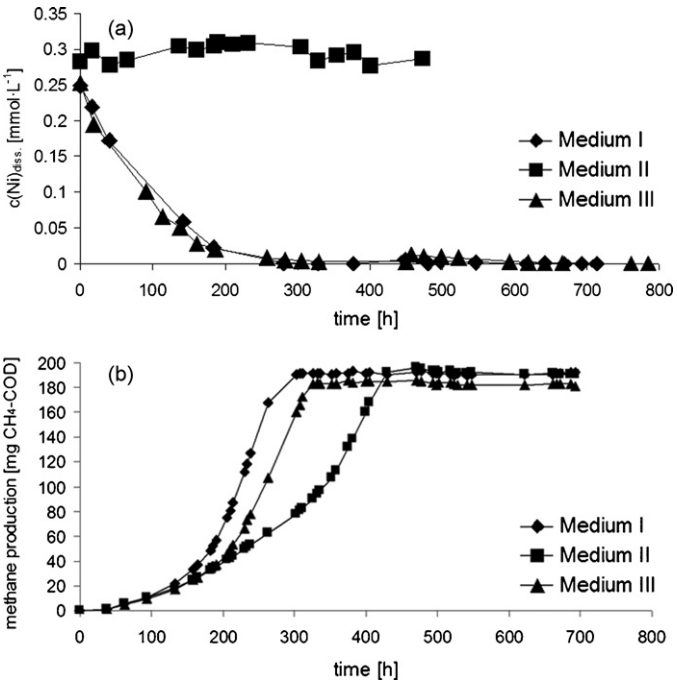

Fig. 1. Example of the kinetics of methane formation and metal dynamics when the granular sludge was fed with methanol in the presence of nickel (0.3 mmol L^{-1}). (a) Kinetics of nickel sorption/precipitation in medium I, II and III. (b) Methane production per bottle by granular sludge incubated in medium I, II and III.

Figs. 1 and 2a shows the kinetics of nickel sorption/precipitation in the three different media for the nickel addition of 0.3 mmol L^{-1}. While the plateau in the nickel concentration was reached immediately in medium II, at least 500 h was needed in media I and III. This was much longer than expected from parallel experiments with cobalt [15] and implies that the process of methane production (in media I and III) took place whilst the nickel concentration was still decreasing (Fig. 1b).

Table 2 gives the kinetic constants and coefficients of determination (R^2) obtained from the pseudo-first order sorption kinetics, pseudo-second order kinetics, first order reversible reaction kinetics and Weber–Morris kinetic models. The pseudo-first order,

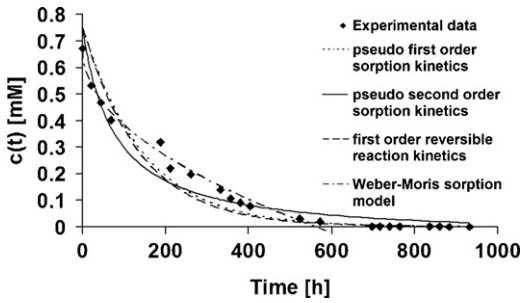

Fig. 2. An example of the measured data fitted with pseudo-first order kinetics, pseudo-second order kinetics, first order reversible reaction kinetics and Weber–Morris plot. The data were measured for an initial nickel concentration of 0.75 mmol L^{-1} in medium III.

Table 2
Kinetic constants and coefficients of determination (R^2) obtained by applying different kinetics models on the data measured with various initial nickel concentrations (c_0) in media I and III.

c_0 [mmol L^{-1}]	Pseudo-first order equation		Pseudo-second order equation		First order reversible reaction model		Weber–Morris model[a]	
	k_1 [h^{-1}]	R^2	k_2 [g mg^{-1} h^{-1}]	R^2	k_r [h^{-1}]	R^2	k_{id} [mg g^{-1} h$^{-1/2}$]	R^2
Medium I								
0.10	0.0113	0.988	0.0047	0.969	0.0127	0.993	0.28	0.979
0.30	0.0117	0.996	0.0014	0.979	0.0110	0.997	0.74	0.972
0.50	0.0094	0.976	0.0010	0.917	0.0118	0.951	0.99	0.995
0.75	0.0097	0.966	0.0011	0.884	0.0096	0.967	1.16	0.998
2.00	0.0112	0.938	0.0010	0.848	0.0078	0.961	1.94	0.990
Medium III								
0.10	0.0093	0.879	0.0061	0.955	0.0113	0.931	0.33	0.991
0.30	0.0099	0.988	0.0019	0.971	0.0103	0.991	0.72	0.995
0.50	0.0103	0.982	0.0011	0.963	0.0110	0.979	1.03	0.993
0.75	0.0062	0.911	0.0006	0.924	0.0082	0.938	1.23	0.989
2.00	0.0037	0.901	0.0005	0.754	0.0029	0.952	1.48	0.962

[a] The data for the Weber–Morris model were derived from the liner part of the Weber–Morris plots as shown in Fig. 3.

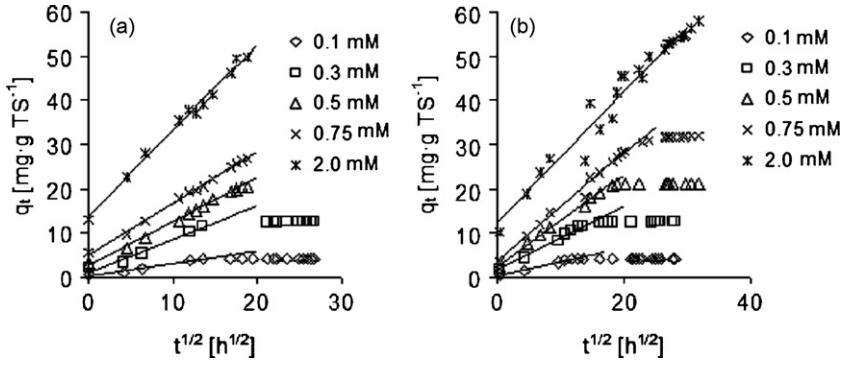

Fig. 3. Weber–Morris plots for nickel sorption in media I (a) and III (b) with the initial nickel concentrations (c_0) of 0.1, 0.3, 0.5, 0.75 and 2.0 mmol L^{-1}.

pseudo-second order and first order reversible reaction kinetics shows very similar and reasonably high R^2 values (0.926–0.986). However, the high R^2 values are given by agreement between the latter models and the experimental data obtained at the end of experiments (at very low nickel concentrations) and none of these models was able to describe sufficiently the decrease of the nickel concentration, especially during the first 400 h (Fig. 2). In contrast, the experimental data could be fitted very well in the period from time 0.2 h (after the initial sorption) up to 100–400 h (depending on the initial nickel concentration) when the steady state was reached with the Weber–Morris model (Figs. 2 and 3). This model considers the intra-particle transport as the limiting step of the sorption process.

Note that the kinetic constant depended on the initial nickel concentrations for all kinetic models used (Table 2). The kinetic constant of the Weber–Morris model increased systematically with the initial nickel concentration in media I and III. Similarly, also the initial sorption (I) increased in both media I and III with increasing initial nickel concentration.

3.1.2. Nickel speciation

As EDTA is a strong ligand, almost all the supplied nickel (89–98%) was always present in solution in the medium containing $[NiEDTA]^{2-}$ (medium II). In contrast, massive sorption/precipitation occurred in media containing $NiCl_2$ with and without phosphates (respectively, medium I and III). Especially with the nickel additions lower than 1 mmol L^{-1}, the concentration in the solution (at the end of both the DMT and the toxicity experiments) was as low as 0.001 mmol L^{-1} and more than 99% of the nickel had precipitated. Comparing the nickel concentrations in media I and III at the end of the toxicity tests, slightly higher (1–3 μmol L^{-1}) values were measured in medium I for additions lower than 1 mmol L^{-1}. In contrast, the end-concentrations of nickel were higher in medium III when 1 and 2 mmol L^{-1} of nickel were added. The dissolved nickel concentrations at the end of the DMT experiments in medium I were higher than in medium III, except for the two lowest nickel additions. The latter was because the dissolved nickel concentrations measured in the DMT experiments in medium I were considerably higher than those measured in the toxicity experiments. In contrast, the dissolved nickel concentrations measured in the DMT experiments in media II and III were approximately as high as those measured in the toxicity experiments using these media.

Fig. 4 shows concentrations of the free nickel ion (Ni^{2+}) at various total dissolved concentrations measured upon the estab-

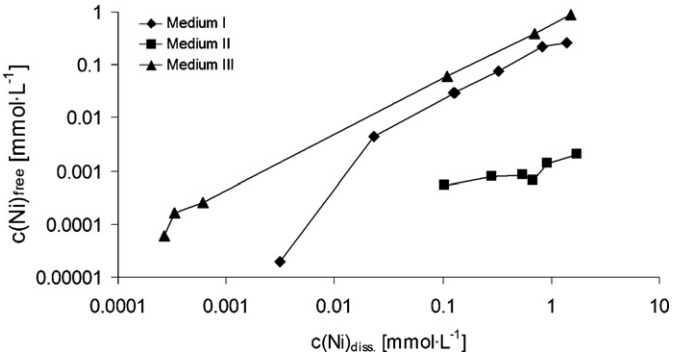

Fig. 4. Concentration of free nickel ion (Ni^{2+}) in medium I, II and III as a function of the total dissolved nickel concentration.

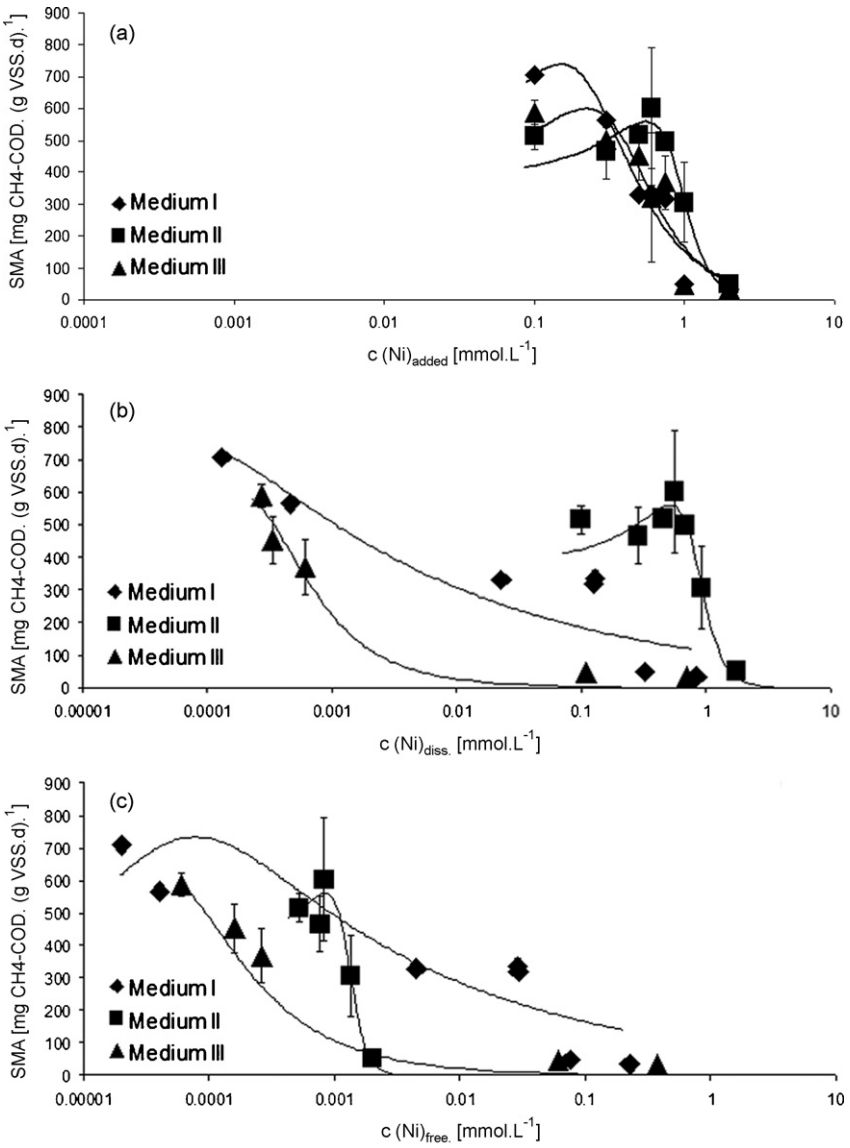

Fig. 5. The SMA obtained under various nickel concentrations in medium I, II and III. The nickel concentration was expressed as total added (a) dissolved (b) and free (c) nickel.

lishment of the sorption equilibrium. The curves show a linear trend with R^2 of 0.95, 0.90 and 1.00 for medium I, II and III, respectively. The average percentage of the abundance of the free ion was 20, 0.1 and 57% for medium I, II and III, respectively. Because the phosphates and EDTA concentration was the only variable between the media I–II, the variations in nickel speciation can be related to these differences in the concentration of these ligands.

3.2. Nickel toxicity to methylotrophic methanogenesis

Two types of batch toxicity experiments were performed in order to examine the effect of the nickel-speciation kinetics: (1) substrate was supplied at the same moment as the nickel dosage and (2) substrate supplied after a pre-incubation (30-day) of the granular sludge in the nickel containing media.

3.2.1. Toxicity of nickel when dosing nickel and methanol simultaneously

When no nickel was added to the medium (Fig. 5), the observed SMA was approximately 40% lower compared to the SMA at the optimal nickel addition (100 μmol L^{-1} for all three media). Nickel additions exceeding the optimal amounts caused a decrease in the SMA of the granular sludge. As Fig. 5a shows, the toxicity of nickel addition in the three media increased in the order: medium II < III < I. The maximal values of the SMA were achieved when 0.1, 0.6 and 0.1 mmol L^{-1} nickel was added to medium I, II and III, respectively. The optimal nickel addition according to the modeled Hormesis curves was 0.16, 0.58 and 0.23 mmol L^{-1} for medium I, II and III, respectively. The IC_{50} value ranged for the three media from 0.48 mmol L^{-1} (medium I) up to 1.05 mmol L^{-1} (medium II). The standard deviation of the IC_{50} value for the total added nickel for the three media was 0.18 mmol L^{-1} (i.e. 19% of the average value).

When the dissolved nickel concentration was taken into account for the calculations, the IC_{50} values ranged from 0.0007 mmol L^{-1} (medium III) up to 0.97 mmol L^{-1} (medium II) and the toxicity of nickel increased in the order: medium II < I < III. The standard deviation between the IC_{50} values for the three media was 0.32 mmol L^{-1} (i.e. 172% of the average value).

When the concentration of the free nickel species was taken in account for the calculations, the IC_{50} values ranged from 0.0002 mmol L^{-1} (medium III) up to 0.0035 mmol L^{-1} (medium I) and the toxicity of nickel increased in the order: medium I < II < III.

Table 3
The SMA_{max} and IC_{50} values obtained from the batch-experiments with correlation coefficient (R^2) for fitting the experimental data with the Hormesis model. The data are supplemented with average value (AVG), relative standard deviation (STDEV) of IC_{50} and SMA_{max} between measurements in the three media (for each nickel fraction).

	Medium I	Medium II	Medium III	AVG	STDEV (%)
Nickel addition					
SMA_{max} (mg CH_4-COD (g VSS)$^{-1}$ d^{-1}	740	560	600	633	15
IC_{50} (mmol L^{-1})	0.84	1.18	0.91	0.97	19
R^2	0.935	0.938	0.865		
Probability that the three toxicity curves are identical			0.7%		
Dissolved nickel					
SMA_{max} (mg CH_4-COD (g VSS)$^{-1}$ d^{-1}	745	560	601	635	15
IC_{50} (mmol L^{-1})	0.089	1.089	0.0012	0.324	172
R^2	0.830	0.940	0.980		
Probability that the three toxicity curves are identical			<0.1%		
Free nickel					
SMA_{max} (mg CH_4-COD (g VSS)$^{-1}$ d^{-1}	735	560	619	638	14
IC_{50} (mmol L^{-1})	0.062	0.0015	0.0005	0.002	97
R^2	0.795	0.951	0.979		
Probability that the three toxicity curves are identical			10%		

The standard deviation between the IC_{50} values for the three media was 0.002 mmol L^{-1} (i.e. 97% of the average value).

The probability (*p*-value) that the three curves could be replaced by one common model curve was <1% in the cases of the total added and dissolved nickel and 10% in the case of free nickel. The slightly higher *p*-value for the free nickel fraction was rather given by the higher deviation in the data on the free ion concentration than by the close similarity of the three curves (Fig. 5c).

3.2.2. Toxicity of nickel after 30-day pre-incubation in a nickel containing media

The SMA values obtained in the second type of the nickel toxicity experiments were comparable with the SMA values obtained without applying a 30-day pre-incubation in media I and III, except for the zero-nickel addition (i.e. control). In contrast, the SMA values obtained in medium II with the 30-day pre-incubation were substantially higher than those obtained previously without a pre-incubation period in the nickel concentration range 0–0.75 mmol L^{-1}.

The same statistical analysis as performed with the first type of toxicity experiments was performed (Fig. 6). Again, no significant similarity between the toxicity curves was found for any of the nickel fractions (Table 3).

4. Discussion

4.1. Prediction of nickel toxicity to anaerobic granular sludge

This study shows that nickel toxicity to methylotrophic methanogenesis by anaerobic granular sludge measured in batch-experiments cannot be estimated based on the concentration of the free nickel species (Ni^{2+}) only: different toxicity curves were obtained for the free nickel fraction in methanogenic test media with a different ligand compositions (Fig. 5c). The reason was that the physical–chemical processes taking place in the methanogenic medium in the presence of anaerobic granular sludge (precipitation, sorption and chemical speciation) were slower than the parallel biological processes (methane production and nickel bio-uptake; Fig. 1). It has been shown previously that the FIAM as well as BLM models are valid when the bio-uptake takes place under nearly equilibrium conditions [1,20]. The latter is fulfilled when the physical–chemical processes in the bulk liquid are faster than the biological processes [1]. As a consequence of the slow precipitation/sorption of nickel in media I and III in the present study, predicting nickel toxicity based on the free ion concentration at steady state fails, i.e. the FIAM cannot be directly applied to predict nickel toxicity in anaerobic granular sludge [7].

Fig. 6 shows that concentrations of the free nickel species measured upon pseudo-equilibrium establishment cannot be used directly to estimate nickel toxicity in the system under investigation. Thus, the free nickel fraction cannot be correlated with nickel toxicity again, as confirmed by the *F*-test (data not shown), even when the methanogenic activity takes place after a stable state was established in the system. Nickel transport into *Methanobacterium*

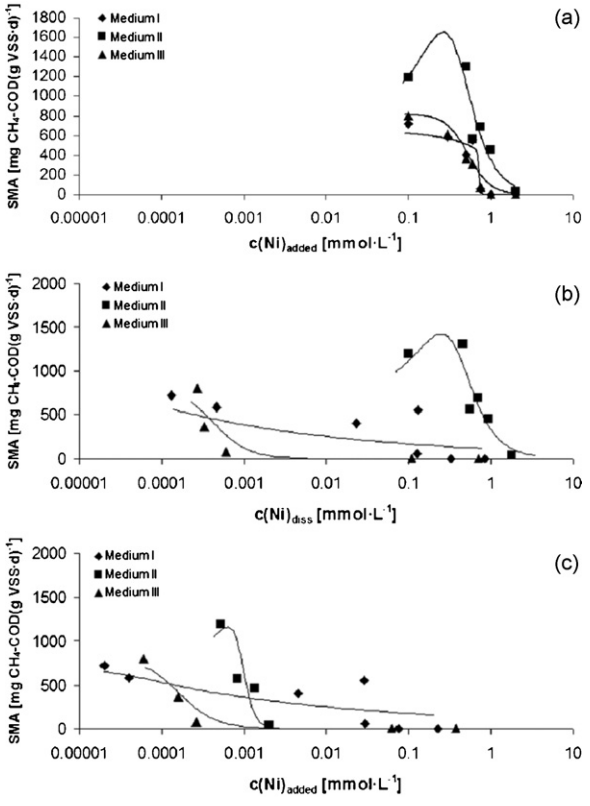

Fig. 6. The SMA obtained under various nickel concentrations in medium I, II and III when the sludge was pre-incubated for 30 days in the nickel containing media prior to the substrate (methanol) supplementation. The nickel concentration was expressed as total added (a) dissolved (b) and free (c) nickel.

bryantii cells occured in maximally 4 h after nickel injection [21]. This indicates that the bio-uptake of nickel (resulting in nickel toxicity) takes place even prior to the start of methanogenic activity, which is much slower than the nickel uptake (several days). Thus the nickel uptake took place independently on the methanogenic activity, well before the chemical equilibrium was established in the medium. The latter was true even when methanol was added only after a pre-incubation period of 30 days (Fig. 6).

4.2. Nickel sorption onto anaerobic granular sludge

4.2.1. Mechanism of nickel sorption onto anaerobic granular sludge

Figs. 2 and 3 show that the process of nickel sorption in anaerobic granular sludge under conditions of media I and III can be partially modeled using the Weber–Morris kinetic model, indicating that intra-particle diffusion acts as the rate-limiting process [14,22]. However, the process consists of three distinctive periods: (1) a fast initial sorption in the first minutes upon nickel injection, (2) a slow sorption process limited by intra-particle diffusion and (3) final equilibrium establishment. Similar interpretation of experimental data as a sequence of steps limited by different processes (initial sorption, intra-particle diffusion and equilibrium establishment) was presented also by Popuri et al. [23] for nickel and cupper sorption in chitosan coated PVC beads or by Vimonses et al. [24] for sorption of organic dyes by clay.

As Fig. 3 shows, a substantial part (in average 16%) of the nickel injected was sorbed almost instantaneously (within 10 min) in the sludge. This initial sorption was proportional to the nickel dosage (Table 2), suggesting that the initial sorption can be related to the adsorption on the easily accessible sorption sides of methanogenic granules such as the surface of the granules [23,25].

Subsequently to the initial sorption, nickel sorption slowed down following the Weber–Morris model (Figs. 2 and 3). Thus, a major part of nickel (at least 80%) is sorbed during a sorption process that is limited by the intra-particle diffusion rate. Note that the sorption rates in this phase of the process were similar in medium I and III (Table 2) indicating that the carbonate and phosphate concentration in the media did not have a substantial effect on the sorption process. The observed increase in the k_{WM} values with increasing initial nickel concentration can be explained by the increasing effect of the driving force resulting in enhanced diffusion of nickel in the solid phase [26].

Finally, when the nickel sorption (q) amounted to 95–99% of the equilibrium sorption (q_e), a third period of the sorption process started that was limited by the low nickel concentrations in the media.

4.2.2. Effect of sorption mechanism on nickel toxicity measured in batch experiments

Nickel toxicity to anaerobic granular sludge, when studied in batch experiments, can only be studied under dynamic conditions, because when toxic dosages of nickel are introduced into methanogenic medium, the sorption process will be slower than the parallel biological processes (nickel bio-uptake, methane production). The latter hinders the prediction of nickel toxicity to anaerobic granular sludge. Van Hullebusch et al. [9] did not observe the slow nickel sorption on a methanogenic granular sludge from the same full-scale UASB reactor as used in this study. However, the latter authors used much greater sludge concentrations (33.2 g TS L^{-1} compared to 1.38 g TS L^{-1} used in this study), resulting in a much lower q_e (up to 6.5 mg g TS^{-1} compared to the range 5–60 mg TS L^{-1} in this study). Thus, the sorption observed by Van Hullebusch et al. [9] corresponds with the initial sorption capacity (I) of the granular sludge as observed in the present study (Table 2). Note that applying such a low nickel/biomass ratio, only negligible amounts of nickel stay in solution (in order of magnitude of μmol L^{-1}), resulting in the absence of nickel toxicity (Fig. 5a and c).

4.3. Effect of 30-day pre-incubation of anaerobic granular sludge in methanol-free methanogenic medium on SMA

The SMA values of the control bottles (without nickel addition) containing media I and III substantially increased (almost to the level of SMA_{max}) after a 30-day pre-incubation period. The latter suggests that the nickel contained in the granules in a non-bioavailable form (e.g. precipitates) was mobilized (by desorption, dissolution, etc.) during the pre-incubation period, reaching the non-limiting concentrations when the methanogenic activity was started. Anaerobic granular sludge indeed contains a stock of non-bioavailable metals [27], which can be released as a consequence of changes in metal speciation induced by environmental changes [28]. Alternatively, the metal speciation can be changed by applying an electro-kinetic treatment [29]. The present study suggests that this pool of essential metals can also be remobilized by pre-incubation in a metal free medium.

4.4. Effect of ligands

The common assumption that complexation decreases heavy metal toxicity [1] was confirmed in the present study: the toxic nickel concentrations (considering the total added nickel) with EDTA present in medium II was substantially higher than the toxic nickel concentrations in the other two media (Table 2). The presence of phosphates in medium I increased substantially the complexation of nickel (Fig. 4), however, this complexation did not decrease the toxic effect of nickel (Fig. 5a). The latter suggests that the nickel complex with phosphates ($[NiHPO_4]$) is either not strong enough to restrict nickel bio-uptake (stability constant according to Visual Minteq – pK = 19.9 compared to $[NiEDTA]^{2-}$ with pK = 20.11) or that the nickel bio-uptake takes place prior to the $[NiHPO_4]$ formation.

5. Conclusions

This study showed that the kinetics of nickel sorption and chemical speciation in the methanogenic granular sludge are crucial for nickel toxicity to methylotrophic methanogens. As shown in the sorption kinetics experiments, the nickel sorption in the methanogenic granular sludge is partially intra-particle diffusion-limited, which results in the slow establishment of the chemical–physical equilibrium in the methanogenic medium. The intra-particle diffusion was confirmed by fitting the experimental data by Weber–Moris model. The results suggest that determination of equilibrium speciation of nickel in the medium studied is not sufficient for estimation of nickel toxicity.

Acknowledgements

This study was funded by the Marie Curie Excellence Grant Novel biogeological engineering processes for heavy metal removal and recovery (MEXT-CT-2003-509567) and the Marie Curie Intra European Fellowship “Bioavailability of trace metals in anaerobic granular sludge reactors” (MEIF-CT-2007-041896).

References

[1] C.S. Hassler, V.I. Slaveykova, K.J. Wilkinson, Environ. Toxicol. Chem. 23 (2004) 283.
[2] G.K. Pagenkopf, Environ. Sci. Technol. 17 (1983) 342.

[3] P.R. Paquin, R.C. Santore, K.B. Wu, C.D. Kavvadas, D.M. Di Toro, Environ. Sci. Policy 3 (2000) 175.
[4] J.H. Campbell, R.D. Evans, Sci. Total Environ. 62 (1987) 219.
[5] P. Sanchez-Marin, J.I. Lorenzo, R. Blust, R. Beiras, Environ. Sci. Technol. 41 (2007) 5679.
[6] H.P. Van Leeuwen, Environ. Sci. Technol. 33 (1999) 3743.
[7] C.S. Hassler, K.J. Wilkinson, Environ. Toxicol. Chem. 22 (2003) 620.
[8] E.D. Van Hullebusch, A. Peerbolte, M.H. Zandvoort, P.N.L. Lens, Chemosphere 58 (2005) 493.
[9] E. Van Hullebusch, M. Zandvoort, P. Lens, J. Chem. Technol. Biotechnol. 79 (2004) 1219.
[10] A. Van der Veen, F.G. Fermoso, P. Lens, Eng. Life Sci. 7 (2007) 480.
[11] C. Oviedo, J. Rodriguez, Quim. Nova 26 (2003) 901.
[12] F.G. Fermoso, J. Bartacek, L.C. Chung, P. Lens, Biochem. Eng. J. 42 (2008) 111.
[13] Y. Liu, Y.-J. Liu, Sep. Purif. Technol. 61 (2008) 229.
[14] J. Febrianto, A.N. Kosasih, J. Sunarso, Y.H. Ju, N. Indraswati, S. Ismadji, J. Hazard. Mater. 162 (2009) 616.
[15] J. Bartacek, F.G. Fermoso, A.M. Baldó-Urrutia, E.D. Van Hullebusch, P.N.L. Lens, J. Ind. Microbiol. Biotechnol. 35 (2008) 1465.
[16] O. Schabenberger, B.E. Tharp, J.J. Kells, D. Penner, Agron. J. 91 (1999) 713.
[17] E.D. Van Hullebusch, M.H. Zandvoort, P.N.L. Lens, Rev. Environ. Sci. Biotechnol. 2 (2003) 9.
[18] M.H. Zandvoort, R. Geerts, G. Lettinga, P.N.L. Lens, Biotechnol. Prog. 18 (2002) 1233.
[19] APHA/AWWA/WEF, Standard Methods for the Examination of Water and Wastewater, American Public Health Association, Washington, DC, USA, 1998.
[20] R.J.M. Hudson, Sci. Total Environ. 219 (1998) 95.
[21] K.F. Jarrell, G.D. Sprott, J. Bacteriol. 151 (1982) 1195.
[22] G. Akkaya, A. Özer, Process Biochem. 40 (2005) 3559.
[23] S.R. Popuri, Y. Vijaya, V.M. Boddu, K. Abburi, Bioresour. Technol. 100 (2009) 194.
[24] V. Vimonses, S. Lei, B. Jin, C.W.K. Chow, C. Saint, Chem. Eng. J. 148 (2009) 354.
[25] R. Krishna Prasad, S.N. Srivastava, J. Hazard. Mater. 161 (2009) 1313.
[26] N.Y. Mezenner, A. Bensmaili, Chem. Eng. J. 147 (2009) 87.
[27] M.H. Zandvoort, E.D. van Hullebusch, J. Gieteling, P.N.L. Lens, Enzyme Microb. Technol. 39 (2006) 337.
[28] F.G. Fermoso, G. Collins, J. Bartacek, P.N.L. Lens, J. Ind. Microbiol. Biotechnol. 35 (2008) 543.
[29] J. Virkutyte, E. van Hullebusch, M. Sillanpaa, P. Lens, Environ. Pollut. 138 (2005) 517.